Mesoscale Variability of Free Troposheric Humidity Near San Nicolas Island During FIRE

A.B. White, C.W. Fairall, and D.W. Thomson
Department of Meteorology
503 Walker Building
Pennsylvania State University
University Park, PA 16802

INTRODUCTION

Humidity variability at the top of the marine boundary layer (MBL) and in the free troposphere has been examined using a variety of measurements taken on and around San Nicolas Island (SNI) during the FIRE IFO in July, 1987. Doppler wind profiler reflectivity recorded at two minute time resolution has provided the most continuous record and detail of small scale humidity fluctuations. Rawinsonde data was available from both an island site and the research vessel Point Sur. The information extractable from these sources is somewhat limited due to the frequency of launches (3-4/day at SNI and 6/day on the Point Sur). Some additional data was available from instrumented aircraft although scheduling flights in the neighborhood of the island was difficult due to restrictions on the air space. Other relevant data was collected at SNI near the radar and rawinsonde launch sites. A continuous record of cloud base altitude was logged by a ceilometer. Doppler acoustic sounder (sodar) reflectivity data provided a good record of inversion height. The sodar also monitored turbulent temperature fluctuations in the MBL. A small ground station recorded hourly averages of solar irradiance and downward longwave irradiance.

This paper describes analysis in progress of the various data sets described above for two adjacent two day periods from 11 July to 14 July. The earlier period was chosen because the marine inversion was unusually high and there was increased frequency of rawinsonde launches at SNI. The later period was chosen because of the significant descent with time of an elevated inversion indicated by the radar data. Throughout the four day period, but especially in the first half, the turbulent humidity structure calculated from Doppler radar reflectivity shows excellent agreement with humidity profiles evaluated from rawinsonde data.

INTERPRETATION OF DOPPLER RADAR REFLECTIVITY

Penn State's Doppler wind profiler used at SNI operates at a frequency of 404.37 MHz. For FIRE, the pulse width was set at 1 μs to provide the best possible range resolution while satisfying the receiver bandwidth constraint. The pulse repetition frequency was 10,000 Hz. Processing of radar reflectivity is accomplished in the following manner. The complex video of 288 consecutive pulses are coherently averaged (time domain integration). A set of 64 of these integrations is processed by a fast fourier transform (FFT) to produce one spectrum. Incoherent averaging is then performed on 8 of these variance spectra to produce the two minute averaged spectrum from which the signal/noise ratio (SNR) is extracted.

Since radar backscatter occurs in a volume (V_s) defined by the pulse and beam widths, volume reflectivity (η) replaces the more familiar backscatter cross-section (σ), where $\eta=\sigma/V_s$. The volume reflectivity is related to the SNR by the spectral radar equation (VanZandt et al., 1978)

$$\eta = \frac{9\pi}{2} \frac{ckB(\alpha T_c + T_{rx})}{\alpha^2 P_t F_r A_p \cos(\chi)} \left(\frac{R}{\Delta R}\right)^2 (SNR), \quad (1)$$

where c is the speed of light, k is Boltzmann's constant, B is the bandwidth of the integrating filter, α is the combined antenna/line efficiency, T_c and T_{rx} are noise temperatures for cosmic noise and the receiver, P_t is the transmitted power, F_r is the pulse repetition frequency, A_p is the antenna area, χ is the off vertical beam axis angle, R is the range, and ΔR is the range resolution. Based on comparison with a previously calibrated 50 MHz Doppler wind profiler located in central Pennsylvania, the overall antenna efficiency was chosen to be 0.18. Additional calibrations of the antenna using aircraft data are currently underway. At λ=0.742 m, $\alpha T_c << T_{rx}$ so to a first approximation cosmic noise interference may be neglected. With the appropriate values inserted, (1) becomes

$$\eta = 7.67 \times 10^{-28} R^2 SNR. \quad (2)$$

The backscatter intensity of the radar's signal depends on the mean refractive index gradient existing in the scattering volume. Therefore, the refractive index structure function parameter (C_n^2) can be written in terms of the radar's volume reflectivity (Ottersten, 1969)

$$C_n^2 = (\eta/0.38)\lambda^{(1/3)}. \quad (3)$$

Insertion of λ=0.742 m and (2) into (3) yields

$$C_n^2 = 1.83 \times 10^{-27} R^2 SNR. \quad (4)$$

Both temperature and humidity fluctuations may contribute to variations in the refractive index within the scattering volume. In radar studies of C_n^2 at low altitudes, the contribution due to temperature fluctuations is usually ignored (Wesley, 1976). Conversion from C_n^2 to C_q^2 is then (following Burk, 1980)

$$C_q^2 = C_n^2 (1667 T^2/P)^2, \quad (5)$$

where T is the temperature and P is the pressure (in mb) within the scattering volume. Combinbing (5) and (4) yields the final form of the equation used to determine C_q^2 from Doppler radar reflectivity;

$$C_q^2 = 5.08 \times 10^{-21} R^2 SNR (T^2/P)^2. \quad (6)$$

RAWINSONDE DATA

During the FIRE IFO, Colorado State University operated a cross-chain Loran atmospheric sounding system (CLASS) at SNI. Scientists from the Naval Postgraduate School launched VIZ Loran-type sondes from the Point Sur. For additional information on the CLASS system and details on processing of the SNI rawinsonde data, see Schubert, et al. (1987a). Water vapor mixing ratio (q) was computed in the standard way.

RESULTS

Fig. 1 shows a time-height cross-section of $\log(C_q^2)$ contours (g/kg) from (6) for July 11-12. In this and the following figures, time in hours is measured continuously starting at 0z on 11 July. Higher values of C_q^2 correspond to regions of increased scattering from turbulent humidity fluctuations. In regions of active turbulence, the structure function parameter (C_x^2) for a particular variable (x) is proportional to the square of the vertical gradient of x (Fairall et al, 1988)

$$C_x^2 = 1.6\gamma_x(C_u^2/N^2)(\partial x/\partial z)^2, \qquad (7)$$

where x could be T, q, or n; C_u^2, a measure of local turbulence, is the velocity structure function parameter, N is the Brunt-Vaisala frequency; and $\gamma_x \supset 0.3$ is a constant. Thus, C_q^2 should correlate well with vertical humidity gradients.

For comparison, Fig. 2 shows q contours (g/kg) derived from rawinsonde data for the same time period shown in Fig. 1. The swath of high $\partial q/\partial z$ across the middle of Fig. 2 is evidence of the MBL inversion height decreasing from about 1000 m at the beginning of 11 July to about 750 m at the end of 12 July. Note that the humidity gradients are well correlated with C_q^2 except for a period from 23z to 29z in which C_q^2 reaches a local minimum while $\partial q/\partial z$ approaches its maximum value.

This apparent disagreement with the relationship in (7) can be analyzed using additional data obtained from the remote sensors located at SNI. A record of cloud base measured by the ceilometer (Schubert et al., 1987b), is shown in Fig. 3. Clear sky is depicted by a point at 960 m. The period labeled 23z to 27z shows a sharp decrease in cloud base, suggesting a period of strong subsidence which eventually leads to clearing just after 27z. Wind speed contours from merged sodar/wind profiler data sets (Syrett, 1988) are shown in Fig. 4. Here, the period from 23z to 29z is characterized by light winds and negligible vertical wind shear. Thus for the period in question, one may conclude that although a strong humidity gradient exists, the mechanisms that would normally generate turbulence in the region of the gradient such as cloud top entrainment and vertical wind shear, are not present, resulting in lower values of C_q^2.

REFERENCES

Burk, S.D., 1980: Refractive index structure parameters: Time-dependent calculations using a numerical boundary-layer model. J. Appl. Meteor., 19, 562-576.

Fairall, C.W., D.W. Thomson, and R. Markson, 1988: An aircraft and radar study of temperature and velocity microturbulence in the stably stratified free troposhpere. Preprint Vol. Eighth Symposium on Turbulence and Diffusion, Amer. Meteor. Soc., Boston, MA, 61-65.

Ottersten, H., 1969: Atmospheric structure and radar backscattering in clear air. Radio Sci., 4, 1179-1193.

Schubert, W.H., P.E. Ciesielski, T.B. McKee, J.D. Kleist, S.K. Cox, C.M. Johnson-Pasqua, and W.L. Smith, Jr., 1987a: Analysis of boundary layer sounding data from the FIRE marine stratocumulus project. Colorado State University Atmospheric Science Paper No. 419, Fort Collins, CO 80523, 101 pp.

Schubert, W.H., S.K. Cox, P.E. Ciesielski, and C.M. Johnson-Pasqua, 1987b: Operation of a ceilometer during the FIRE marine stratocumulus project. Colorado State University Atmospheric Science Paper No. 420, Fort Collins, CO 80523, 34 pp.

Syrett, W.J., 1988: Hourly wind, potential temperature and Richardson number profiles at San Nicolas Island during project FIRE. FIRE Technical Report No. 2, Dept. of Meteor., Pennsylvania State University, University Park, PA 16802, 49 pp.

VanZandt, T.E., J.L. Green, K.S. Gage, and W.L. Clark, 1978: Vertical profiles of refractivity turbulence structre constant: Comparison of observations by the Sunset Radar with a new theoretical model. Radio Sci., 13, 819-829.

Wesely, M.L., 1976: The combined effect of temperature and humidity fluctuations on refractive index. J. Appl. Meteor., 15, 43-49.

Acknowledgements. This work is supported by ONR contract N00014-86-K-0688. The authors wish to express special thanks to Bob Peters, Dick Thompson, and Scott Williams of the Department of Meteorology, PSU, for their part in the development and installation of PSU instrumentation at SNI.

Fig. 1 Time-height cross-section of $\log(C_q^2)$ contours (g/kg) calculated from Doppler radar reflectivity.

Fig. 2 Time-height cross-section of specific humidity contours (g/kg) from rawinsondes launched at SNI. Data was compiled by Schubert et al., (1987a).

Fig. 3 Filtered cloud base versus time from ceilometer data collected at SNI during FIRE (after Schubert et al., 1987b). Clear sky is depicted by a point at 960 m.

Fig. 4 Time-height cross-section of wind speed contours (m/s) derived from merged sodar/wind profiler data sets (after Syrett, 1988).

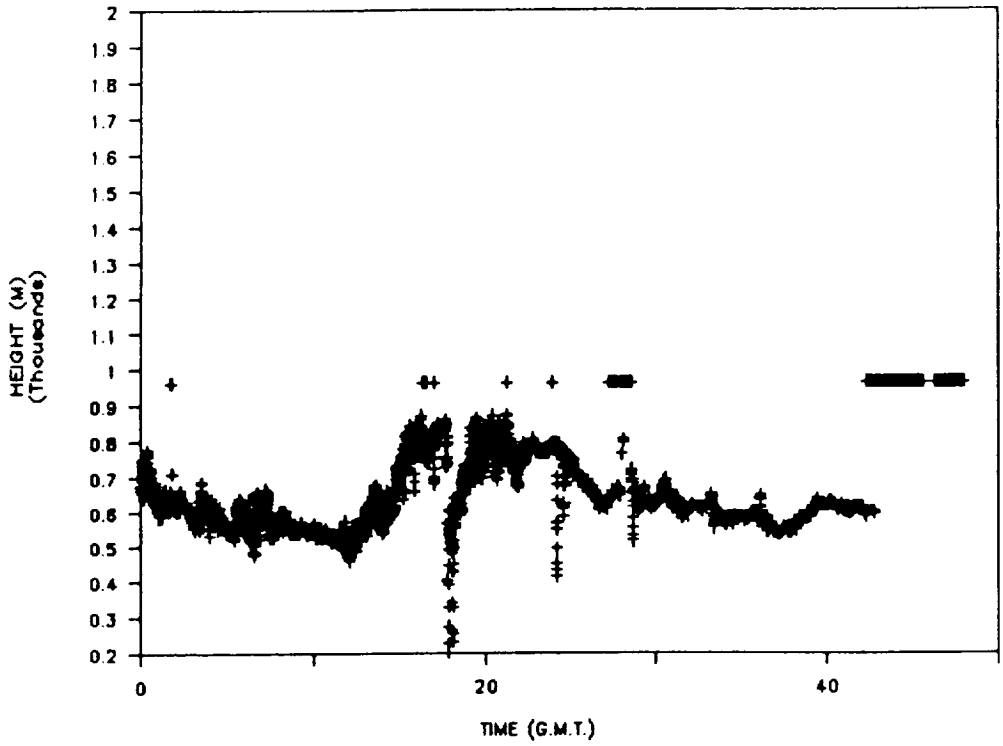

Fig. 3 Filtered cloud base versus time from ceilometer data collected at SNI during FIRE (after Schubert et al., 1987b). Clear sky is depicted by a point a 960 m.

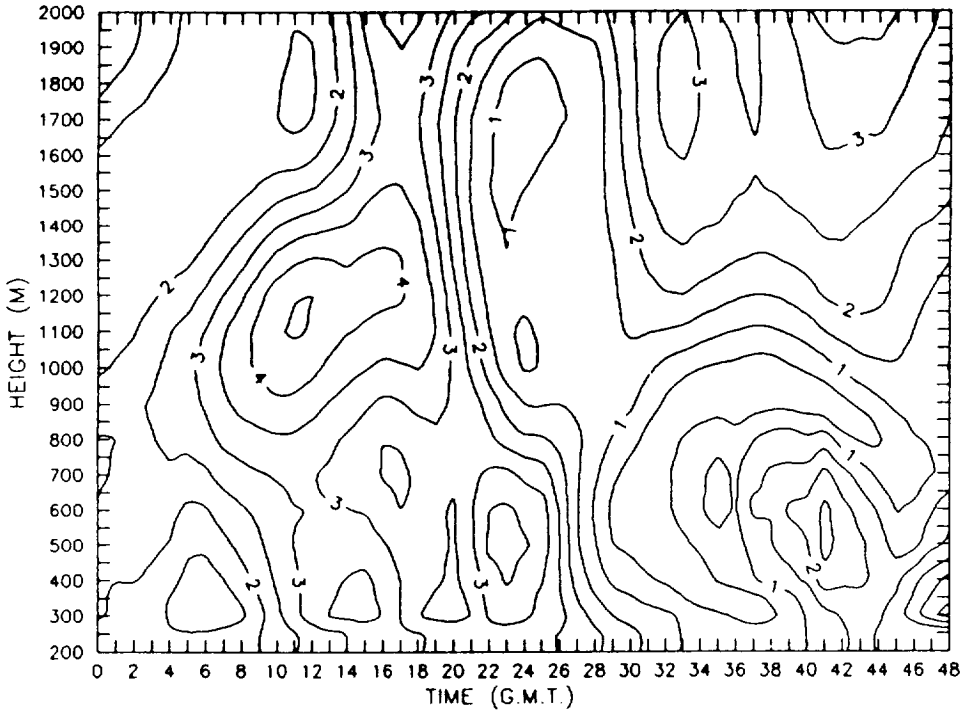

Fig. 4 Time-height cross-section of wind speed contours (m/s) derived from merged sodar/wind profiler data sets (after Syrett, 1988).

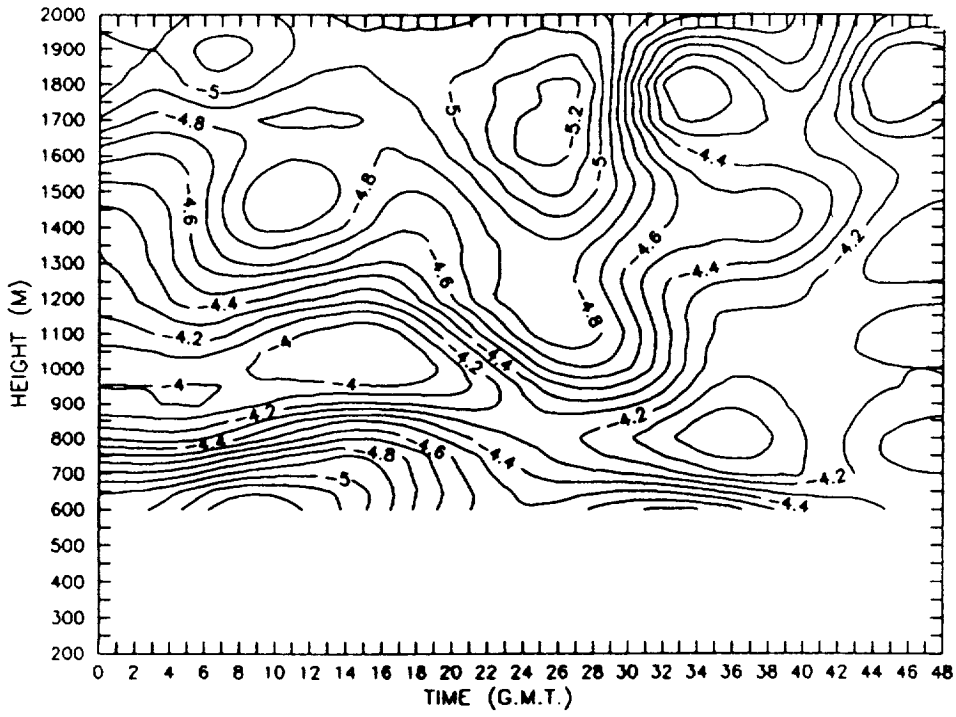

Fig. 1 Time-height cross-section of $\log(C_q^2)$ contours (g/kg) calculated from Doppler radar reflectivity.

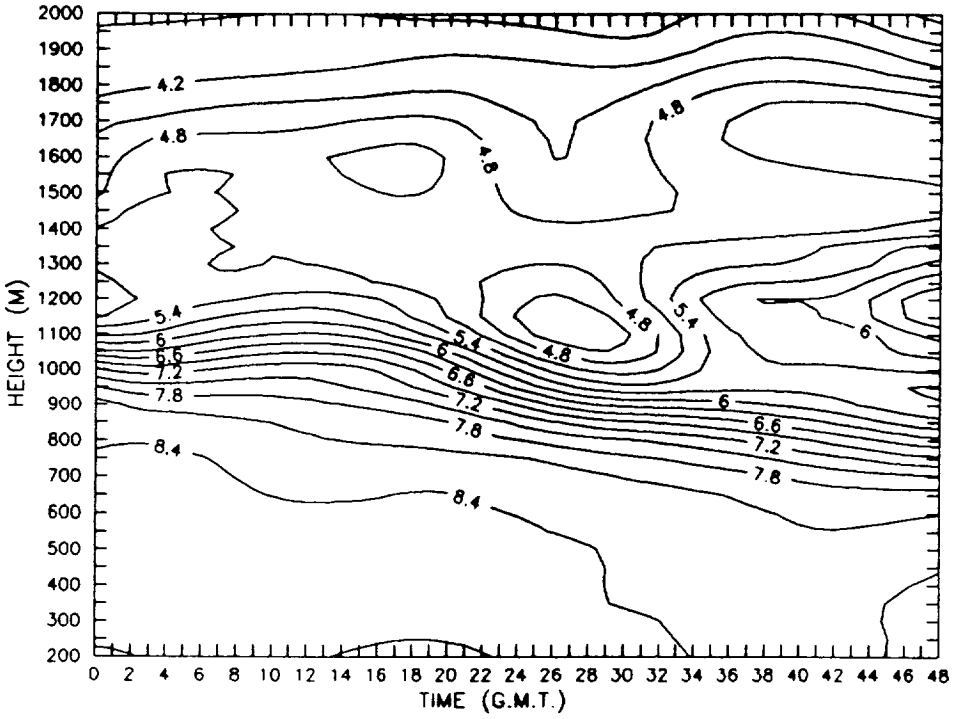

Fig. 2 Time-height cross-section of specific humidity contours (g/kg) from rawinsondes launched at SNI. Data was compiled by Schubert et al., (1987a).